INTERNATIONAL JOURNAL OF ROBOTICS
(THEORY AND APPLICATIONS)
E-mail: IJR@kntu.ac.ir

Planning and Control of Two-Link Rigid Flexible Manipulators in Dynamic Object Manipulation Missions

B. Tarvirdizadeh [a,*], K. Alipour [b]

[a] Department of Mechatronics Eng., Faculty of New Sciences and Technologies, University of Tehran, Tehran, Iran, P.O. Box, 14399-57131
[b] Department of Mechatronics Eng., Faculty of New Sciences and Technologies, University of Tehran, Tehran, Iran, P.O. Box, 14399-57131

ARTICLE INFO

Article history:

Received: June 23, 2015.
Received in revised form:
October 18, 2015.
Accepted: October 25, 2015

Keywords:

Dynamic object manipulation
Optimal trajectory planning
Pseudospectral method
Rigid flexible manipulators

ABSTRACT

This research focuses on proposing an optimal trajectory planning and control method of two link rigid-flexible manipulators (TLRFM) for Dynamic Object Manipulation (DOM) missions. For the first time, achievement of DOM task using a rotating one flexible link robot was taken into account in [20]. The authors do not aim to contribute on either trajectory tracking or vibration control of the End-Effector (EE) of the manipulator; On the contrary, utilizing the powerful tool optimal control accomplishing a point-to-point task for TLRFM is the purpose of the current research. Towards this goal, the pseudospectral method will be developed to meet the optimality conditions subject to system dynamics and boundary conditions. The complicated optimal trajectory planning is formulated as a nonlinear programming problem and solved by SNOPT nonlinear solver. To make robust the response of optimal control against external disturbances as well as model parameter uncertainties, the control partitioning concept is employed. The controlled input is composed of an optimal control-based feedforward part and a PID-based feedback component. The obtained simulation results reveal the usefulness and robustness of the developed composite scheme, in DOM missions.

1. Introduction

Agile maneuvers and a higher ratio of payload to arm weight are some dominant benefits of flexible-link manipulators over the rigid ones. As a result, over the past two decades, extensive research has been performed regarding the control of flexible robots. In particular, great attention has been paid to the control of single-link flexible robots. However, it is difficult to use these robots in practical application. Single-link flexible robots have only one-dimensional workspaces. In contrast to single-link manipulators, Two-Link Flexible Manipulators (TLFMs) provide more dexterity and offer two-dimensional workspaces. However, their first link has very low torsional stiffness, which normally causes torsional vibrations in addition to transversal vibrations [1]. Hence, some researchers and designers may prefer to replace the first flexible link of the TLFMs by a rigid member which results in a TLRFM structure.

In [2] the modeling and control of a TLRFM is outlined. The flexible-link is considered as an Euler-Bernoulli beam with a mass connected at its free end as a payload. Two control schemes are applied to achieve regulation for the joints of the system and for the tip of the flexible-link. These control schemes are the so-

*. Corresponding address: Department of Mechatronics Eng., Faculty of New Sciences and Technologies, University of Tehran, Tehran, Iran,
Tel.: +98 2161115775; fax: +982188497324, Email address: bahram@ut.ac.ir.

called passivity-based velocity feedback and strain-feedback schemes. Finally, some simulation results are presented for both control schemes in which it can be seen that the system has a better performance when the strain feedback control scheme is used.

An optimal trajectory planning technique for suppressing residual vibrations in TLRFM is proposed in [3]. The equations of motion of the manipulator are derived using the Lagrangian approach and the assumed modes method. For the trajectory planning, the joint angle of the flexible link is expressed as a cubic spline function, and then the particle swarm optimization algorithm is used to determine the optimal trajectory. The optimal trajectory thus obtained satisfies the minimum vibration condition.

Two distributed controllers for a TLRFM were presented in [4]. The first distributed controller uses three PD-like fuzzy logic controllers. The second distributed controller is based on evaluating the importance degrees of the output variables of the system. The parameters in both controllers were tuned using nonlinear programming to obtain better performance. The robustness of both tuned distributed controllers was tested by varying the joint trajectories and angular velocities. The effect of changing the payload on the robustness of the two controllers was also considered.

As described above, the aforementioned researches aim to control the end-effector motion to track a predefined trajectory and/or to suppress its vibration. In contrast, the aim of the current study is neither trajectory tracking control nor vibration suppression of TLRFM, but instead, it attempts to control its motion to successfully throw the object at a specified point with a desired known velocity. It is worth mentioning that the object throwing task is a special kind of a wide object manipulation mission category, known as *Graspless Manipulation*.

Nonprehensile or Graspless Manipulation (GM) as an important research topic has some advantages such as no bearing of the object's total weight, use of simple robots to control the object, handling of the object where grasping is impractical [5, 6].

In GM, simple mechanisms are used to deal with the dynamics and the geometry of the environment and object [7].

One of the disadvantages of the GM is the complexity in planning [8]. GM may be impossible to be reversed [9].

Quasi-static and dynamic manipulations are two major different categories in GM. Loss of contact between the manipulator and the object in some manipulation intervals is allowed in dynamic manipulation [10].

Handling of a planar rigid body on a conveyor belt via a robot containing just one joint studied by Akella et al. [11]. Pushing paths planning by stable pushes problem studied by Lynch and Mason [12].

Controllability description, application of planar dynamic GM, and motion planning is the other works of the Lynch and Mason [13].

Tabata and Aiyama have studied problem of tossing using one-degree-of-freedom robot [14]. DOM problem containing of throwing and catching a disc via two planar manipulators is analyzed in [15]. Akbarimajd et al. [16] studied polygonal objects manipulation using one revolute joint robot from planning and kinematics points of view. Strategy of throwing mission for one-degree-of-freedom robot proposed by Miyashita et al. [17]. A novel issue in object manipulation strategy by a dual soft-fingered robotic hand system, and also another novel strategy to control the position and orientation of the object via triple soft-fingered robotic hand system in the task space are proposed by Tahara et al in [18] an [19], respectively.

The authors have already proposed a novel issue in the area of DOM [20] considering the use of a rotating one-link flexible manipulator. In the present research, the authors have more improved the previous work to propose an *optimal trajectory planning method* for *two link rigid-flexible manipulators* in DOM missions. The *pseudospectral method* will be developed to satisfy optimality conditions subject to system dynamics and path constraints. The aim of the TLRFM, in the current study, is to launch an object from an arbitrary specified position in *xy*-plane to a predetermined arbitrary position with the considered velocity vector. It is worth mentioning that the object's end position may be out of the work-space of the robot. It is stressed that this research plans to target neither trajectory tracking nor vibration control of the EE of flexible robots as there are a lot of researches that have addressed these up to now [21-22] but rather on DOM by TLRFM which may utilizes the flexural properties of the robot to increase the considered performance. Herein, however, simultaneous EE velocity and position vectors control of a TLRFM in the limited and specified time has been put in perspective as the objective of control problem. EE velocity and position vectors control is an under-actuated problem because the numbers of control inputs are less than the degrees of freedom of the system.

After the previous explanation on the problem, in section 2, the robotic system model is explained and the system nonlinear model will be derived. The DOM problem formulation and its solution procedure will be discusses in section 3. In section 4, the application of proposed scheme to find the time-history of the control inputs is provided for a considered TLRFM. In section five a hybrid control structure is elaborated to provide the system robustness. Some concluding remarks are mentioned at the final section.

2. System Modeling

In the current segment, the TLRFM nonlinear model is derived, for movement in horizontal plane. The TLRFM schematic, with the first rigid link and the other flexible one, is depicted in Figure 1. The density of the first link is much higher than the second one. All later used parameters are described in Table 1. The Flexible Link (FL) is assumed to modeled as an Euler–Bernoulli beam. It is recalled that in the later analyses, the transverse deflection of the FL is only considered and modeled.

The position vectors of any arbitrary point on the first link, its tip, any arbitrary point on the second link and EE of the TLRFM, in the XY coordinate frame, could be derived as follows, respectively:

$$\mathbf{P_1} = (O_{h1} + x_1)\vec{i}_1$$
$$\mathbf{P_{t1}} = (O_{h1} + l_1 + O_{t1})\vec{i}_1$$
$$\mathbf{P_2} = \{(L_1) + (O_{h2} + x_2)\cos(\theta_2) - y\sin(\theta_2)\}\vec{i}_1 + \{(O_{h2} + x_2)\sin(\theta_2) + y\cos(\theta_2)\}\vec{j}_1 \quad (1)$$
$$\mathbf{P}_e = \begin{bmatrix} \{L_1 + L_2\cos(\theta_2) - Y_a\sin(\theta_2)\}\vec{i}_1 \\ + \{L_2\sin(\theta_2) + Y_a\cos(\theta_2)\}\vec{j}_1 \end{bmatrix}$$

Also, the velocity vectors of any arbitrary point on the first link, its tip, any arbitrary point on the second link and EE of the TLRFM, in the XY coordinate frame, could be written as follows, respectively:

$$\mathbf{V_1} = (O_{h1} + x_1)\dot{\theta}_1\vec{j}_1$$
$$\mathbf{V_{t1}} = (O_{h1} + l_1 + O_{t1})\dot{\theta}_1\vec{j}_1$$
$$\mathbf{V_2} = -\begin{Bmatrix} (O_{h2} + x_2)\dot{\theta}_1\sin(\theta_2) + \\ \dot{y}\cos(\theta_2) + \dot{y}\sin(\theta_2) \end{Bmatrix}\vec{i}_1 \begin{Bmatrix} (O_{h2} + x_2)\dot{\theta}_1\cos(\theta_2) + \dot{y}\cos(\theta_2) \\ -\dot{y}\sin(\theta_2) + (O_{h1} + l_1 + O_{t1})\dot{\theta}_1 \end{Bmatrix}\vec{j}_1 \quad (2)$$
$$\mathbf{V}_e = -\{(L_2)\dot{\theta}_1\sin(\theta_2) + Y_a\dot{\theta}_1\cos(\theta_2) + \dot{Y}_a\sin(\theta_2)\}\vec{i}_1 \{(L_2)\dot{\theta}_1\cos(\theta_2) + \dot{Y}_a\cos(\theta_2) - Y_a\dot{\theta}_1\sin(\theta_2) + (L_1)\dot{\theta}_1\}\vec{j}_1$$

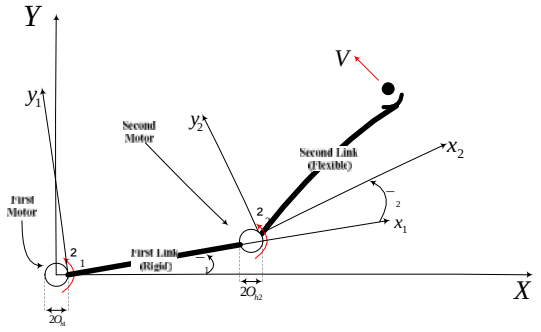

Figure 1. The TLRFM schematic

Table 1. Parameters Definitions, Mechanical Parameters and Physical Specifications of the TLRFM

Symbol	Explanation	Quantity	Unit
l_i	links length (j=R,F[1])	131	cm
c_i	links width	5	cm
b_j	links[2] thickness	3 4.5	mm
m_{li}	links mass per length	1.179	kg/m
m_{O_i}	object mass	.2	kg
τ_i	motor applied torque		N.m
E	elastic modulus	206e9	Pa
m_{hi}	hub mass	300	gr
I_2	moment of inertia of the cross-section of the FL	379.7	mm^4
I_{h_j}	rotational inertia of the hub	0.142	$kg.m^2$
O_{t_j}	tip offset from its center	3 0	cm
I_{t_j}	rotational inertia of the tip	0.0139 24e-5	$kg.m^2$
m_{t_j}	tip masses	0.4 0.2	kg
O_{h_j}	root to joint center offset	3 0	m
$q_{bi}(t)$	FL generalized coordinate	-	-
$\phi(x)$	FL mode shapes	-	-
Q	Work of generalized force	-	-

[1]. "R" stands for the rigid link and "F" stands for the FL.

[2]. The values in the first and the second rows for some parameters correspondent to the rigid and FL, respectively.

where $\vec{i}_1 = [\cos(\theta_1) \quad \sin(\theta_1)]^T$, $\vec{j}_1 = [-\sin(\theta_1) \quad \cos(\theta_1)]^T$, $\dot{y} = \frac{\partial}{\partial t}y(x_2,t)$, $\dot{Y} = \frac{\partial}{\partial t}y(l_2,t)$, $Y_a = y(l_2,t) + O_{t2}\cdot y'(l_2,t)$, $L_1 = l_1 + O_{h1} + O_{t1}$, $L_2 = l_2 + O_{h2} + O_{t2}$, $\theta = \theta_1 + \theta_2$; meanwhile, $y = y(x_2,t)$ is the flexural displacement of the FL, and $Y = y(l_2,t)$ denotes the displacement of the FL tip, in the rotating, $x_2 - y_2$, coordinate frame, and $Y' = \partial(y(x_2,t))/\partial x_2\big|_{x_2=l_2}$.

A brief simplification is done and the first three elastic dominated modes of the FL are considered to approximate $y(x,t)$ via assumed modes method, as,

$$y(x,t) = \sum_{i=1}^{n}\phi_i(x)\cdot q_{bi}(t) \ , \ n = 3 \quad (3)$$

where the boundary conditions of the clamped-free have been considered for $y(x,t)$. n is the number of considered mode shapes ($\ddot{\phi}_i(x)$) for FL in this research. The Euler-Bernoulli equation for the FL is given as follows

$$EI \cdot \frac{\partial^4 (y(x,t))}{\partial x^4} + m_l \cdot \frac{\partial^2 (y(x,t))}{\partial t^2} = 0 \tag{4}$$

The mode shapes associated with clamped-free boundary conditions can be introduced as follows [23].

$$\begin{aligned} \ddot{\phi}_i(x) &= A_1 \cos(\alpha_i x) + A_2 \sin(\alpha_i x) \\ &+ A_3 \cosh(\alpha_i x) + A_4 \sinh(\alpha_i x) \end{aligned} \tag{5}$$

where $\alpha_i^4 = \mu_i^2 \cdot m_l / EI$. Also μ_i which represents the *i*-th natural frequency of the flexible link is as follow

$$\mu_i^2 = EI \cdot \int_0^l \left(\frac{d^2 (\ddot{\phi}_i(x))}{dx^2} \right)^2 dx \qquad i = 1, ..., 3 \tag{6}$$

Based on the given values in Table 1, the following relations can be derived for 3 mode shapes of the FL

$$\begin{aligned} \ddot{\phi}_1(x) &= 0.571136 \times \begin{pmatrix} 1.3146\ \cos(1.196x) - \sin(1.196x) \\ -1.3146\ \cosh(1.196x) + \sinh(1.196x) \end{pmatrix} \\ \ddot{\phi}_2(x) &= 0.7958 \times \begin{pmatrix} 0.9872 \cos(3.216x) - \sin(3.216x) \\ -0.9872 \cosh(3.216x) + \sinh(3.216x) \end{pmatrix} \\ \ddot{\phi}_3(x) &= 0.791866 \times \begin{pmatrix} 1.0004 \cos(5.535x) - \sin(5.535x) \\ -1.0004 \cosh(5.535x) + \sinh(5.535x) \end{pmatrix} \end{aligned} \tag{7}$$

To derive the system model through Lagrangian formalism, the system potential and kinetic energies should be computed. Therefore, the kinetic energy of the system is derived which involves 6 parts and can be written as follows

$$\begin{aligned} T_1 &= \frac{1}{2} m_{l_1} \int_0^{l1} \left\{ (O_{h1} + x_1) \dot{\theta}_1 \right\}^2 dx_1 \\ T_2 &= \frac{1}{2} m_{l2} \int_0^{l2} \{ \mathbf{V_2} \cdot \mathbf{V_2} \} dx_2 \\ T_3 &= \frac{1}{2} I_{h1} \dot{\theta}_1^2 \\ T_4 &= \frac{1}{2} I_{t1} \dot{\theta}_1^2 + \frac{1}{2} m_{t1} L_1^2 \dot{\theta}_1^2 \\ T_5 &= \frac{1}{2} I_{h2} \dot{\theta}_2^2 + \frac{1}{2} m_{h2} L_1^2 \dot{\theta}_1^2 \\ T_6 &= \frac{1}{2} m_{t2} (\mathbf{V}_e \cdot \mathbf{V}_e) + \frac{1}{2} I_{t2} \cdot \left(\dot{\theta}_2 + \dot{y}'(x_2 = l_2, t) \right)^2 \\ E_{kin} &= T_1 + T_2 + T_3 + T_4 + T_5 + T_6 \end{aligned} \tag{8}$$

where T_1 and T_2 are the kinetic energy of the first and second links, respectively. Also, T_3 and T_5 are the kinetic energy of the first and second joint hubs, respectively. Besides, T_4 and T_6 are the kinetic energy of the first and second link tip masses, respectively. It is worth mentioning that $\boldsymbol{V}_2.\boldsymbol{V}_2$ is as follow.

$$\begin{aligned} \mathbf{V_2} \cdot \mathbf{V_2} &= (O_{h2} + x_2)^2 \dot{\theta}_1^2 + (\dot{y}\dot{\theta}_1)^2 + (\dot{y})^2 + (L_1 \dot{\theta}_1)^2 \\ &+ 2\dot{y}\dot{\theta}_1 (O_{h2} + x_2) + 2L_1 \dot{\theta}_1 \dot{\theta}_1 (O_{h2} + x_2) \cos(\theta_2) \\ &- 2L_1 \dot{\theta}_1 \dot{\theta}_1 y \sin(\theta_2) + 2L_1 \dot{\theta}_1 \dot{y} \cos(\theta_2) \end{aligned} \tag{9}$$

The system's potential energy can be derived as

$$E_{pot} = \frac{1}{2} EI_2 \int_0^{l_2} \left(\frac{\partial^2 (y(x_2,t))}{\partial x_2^2} \right)^2 dx_2 \tag{10}$$

The virtual works of the generalized forces on the system can be define as

$$\delta W = \tau_1 \delta \theta_1 + \tau_2 \delta \theta_2 \tag{11}$$

where τ_1 and τ_2 are the first and the second motor applied torques. Substituting Eqs. 8,10-11 into the Lagrange equations leads

$$\mathbf{M}(\mathbf{q})\ddot{\mathbf{q}} + \mathbf{V}(\mathbf{q}, \dot{\mathbf{q}}) = [\tau_1, \tau_2, 0, 0, 0]^T \tag{12}$$

where $\mathbf{q} = [\theta_1, \theta_1, q_{b1}, q_{b2}, q_{b3}]^T$, indicates the system generalized coordinate, $\mathbf{M}(\mathbf{q})$ is the mass/inertia matrix of the robot and $\mathbf{V}(\mathbf{q}, \dot{\mathbf{q}})$ represents the terms containing $\mathbf{q}$ and/or $\dot{\mathbf{q}}$ of the robot dynamics equation. The governing dynamic equations of motions of the system can be divided into a set of five nonlinear, coupled, stiff, second-order ordinary differential equations. The obtained equations are then transcribed into a set of 10 first-order ordinary differential equations, i.e. the state space style, to facilitate the controller design. The state vector $\mathbf{x}$ is defined as:

$$\begin{aligned} \mathbf{x} = [& x_1 \ \ x_2 \ \ x_3 \ \ x_4 \ \ x_5 \ \ x_6 \ \ x_7 \ \ x_8 \ \ x_9 \ \ x_{10}]^T = \\ & [\theta_1 \ \ \theta_2 \ \ q_{b_1} \ \ q_{b_2} \ \ q_{b_3} \ \ \dot{\theta}_1 \ \ \dot{\theta}_2 \ \ \dot{q}_{b_1} \ \ \dot{q}_{b_2} \ \ \dot{q}_{b_3}]^T \end{aligned} \tag{13}$$

The state space equations of the system can be obtained as

$$\dot{\mathbf{x}} = \mathbf{f}(\mathbf{x}(t), \mathbf{u}(t)) \tag{14}$$

where $\mathbf{u} = [\tau_1 \ \ \tau_2]^T$ and $\mathbf{f}(\mathbf{x},\mathbf{u})$ is a 10 by one column vector function in terms of $\boldsymbol{x}$ and $\boldsymbol{u}$, as

$$\mathbf{f} = \left[x_6, x_7, x_8, x_9, x_{10}, \mathbf{M}^{-1}(\boldsymbol{\tau} - \mathbf{V}) \right]^T \tag{15}$$

The above obtained dynamics has been simulated in Maple software. The obtained results were in close agreement with those of [24-26], which ascertained the authors about the soundness of the obtained equations of motion.

3. Formulation of DOM problem and its solution

3.1. DOM Problem Formulation

Design of the optimal path of a TLRFM is the main aim of this paper for executing the desired DOM mission. For the first time in [20], the problem of DOM

by a one link flexible arm for a specified time-duration was examined. However, in the current study the two link rigid-flexible one is considered. The goal of the current study is launching a pre-captured object from rest pose $\boldsymbol{x} = \mathbf{0}$ at a desired coordinate (X_{des} , Y_{des}) with a predetermined velocity ($\dot{X}_{des}$, $\dot{Y}_{des}$) within a specified time. Note that it has assumed the object has rigidly connected to the EE before launching time interval, via a magnetic holder. This holder releases the object at the launch instant.

To tackle such a complicated problem a powerful optimal control strategy is adopted.

To design the optimal trajectories and control input, first a cost function is founded, which is herein considered to be the control effort for the desired DOM task plus penalty term indicates the sensitivity to the terminal conditions, as

$$J = h\left(\mathbf{x}(t_f), t_f\right) + \frac{1}{2}\int_{t_0}^{t_f}\left(\mathbf{u}^T \boldsymbol{\alpha}\, \mathbf{u} + \mathbf{x}^T \mathbf{S}\, \mathbf{x}\right) dt \tag{16}$$

$$\begin{aligned} h\left(\mathbf{x}(t_f), t_f\right) = {} & \frac{1}{2}\left(\mathbf{P}_{des}^f - \mathbf{P}_e(t_f)\right)^T \mathbf{W}_P \left(\mathbf{P}_{des}^f - \mathbf{P}_e(t_f)\right) \\ & + \frac{1}{2}\left(\mathbf{V}_{des}^f - \mathbf{V}_e(t_f)\right)^T \mathbf{W}_V \left(\mathbf{V}_{des}^f - \mathbf{V}_e(t_f)\right) \end{aligned} \tag{17}$$

where $\mathbf{P}_{des}^f$ and $\mathbf{V}_{des}^f$ denote the desired position and velocity of EE of robot manipulator, respectively. Additionally, $\mathbf{P}_e\left(t_f\right)$ and $\mathbf{V}_e\left(t_f\right)$ indicate the real position and velocity of EE of robot manipulator at final time (t_f), respectively. Also, $\mathbf{W}_P$ and $\mathbf{W}_V$ are user-defined semi positive definite matrices representing the relative significance of each error term. It is pointed out that in Eqs. 16, 17, the user-defined positive definite matrix $\boldsymbol{\alpha}$ determines the relative importance between control effort and final errors of position/velocity of the EE. Matrix **S** is a semi positive definite matrix. Notice that the quadratic term versus **x** in equation 16 was added to the control effort in the integrand so as, the constrains on the state vector are satisfied and its shape can be formed in the desired manner. For instance by adopting this approach, strict limitations on the FL deflection and joint angles can be fulfilled.

3.2. Solution of the Considered Optimal Control Problem

Since the complexity of engineering problems, have been increased over the past two decades, the optimal control subject, has transitioned from theory to computation, and variety of numerical methods and corresponding software have been developed and implemented. There are two main procedures to solve the optimal control problems including direct and indirect search approaches.

In this research, a direct search method based on Radau pseudo-spectral method has been utilized for solution of the considered nonlinear optimal control problem. During the last decade, *pseudospectral methods*, based on direct collocation method, have risen to fame in the numerical solution of optimal control problems [27]. The state and control vectors are approximated using global polynomials and collocation of the differential-algebraic equations is performed at *orthogonal collocation points*, in Pseudospectral method. This method is the *combination* of using global polynomials with orthogonally collocated points, are known to converge spectrally [27].

In order to solve the problem based on [27], the following time space transformation is required to map the time interval of $t \in \left[t_0, t_f\right]$ to the new one of $\tau \in [-1, 1]$.

$$\tau = \frac{2t}{t_f - t_0} - \frac{t_f + t_0}{t_f - t_0} \tag{18}$$

Now, employing this transformation the whole problem containing the performance index, states, controls and constraints should be rewritten in term of variable τ according to above transformation. According to the Pseudospectral method, to estimate **x**, in the transformed time interval $\tau \in [-1,1]$, this mapped time interval must be discretized. The division number is *K* and the obtained relevant points known as *Legendre-Gauss* (LG) points. Considering the LG points plus the points $\tau_0 = -1$ and $\tau_{K+1} = 1$, the state variables will be approximated using *K+1* Legendre polynomial L_i, which is as [28]:

$$\mathbf{x}(\tau) \approx \mathbf{X}(\tau) = \sum_{i=0}^{k} L_i(\tau)\, \mathbf{X}(\tau_i) \tag{19}$$

where

$$L_i(\tau) = \prod_{j=0, j\neq i}^{k} \frac{\tau - \tau_j}{\tau_i - \tau_j} \tag{20}$$

where $\mathbf{X}(\tau)$ is approximation of $\mathbf{x}(\tau)$ at point τ_i. Also, control vector is estimated according to *K* Lagrange polynomials as

$$\mathbf{u}(\tau) \approx \mathbf{U}(\tau) = \sum_{i=0}^{k} L_i(\tau)\, \mathbf{U}(\tau_i) \tag{21}$$

where $\mathbf{U}(\tau_i)$ is approximation of $\mathbf{u}(\tau)$ at point τ_i. Next step is reconstruction of dynamical constraints as follow:

$$\begin{aligned} & \sum_{i=0}^{k} D_{ki}(\tau)\, \mathbf{X}(\tau_i) - \frac{t_0 - t_f}{2}\mathbf{f}\left(\mathbf{X}(\tau_k), \mathbf{U}(\tau_k), \tau_k; t_0, t_f\right) \\ & \qquad (k = 1, \ldots K) \end{aligned} \tag{22}$$

where '**D**' is a pseudo-spectral differentiation matrix of *K×(K+1)* dimension. '**D'** contains Legendre polynomial differentiation at collocation points which can be calculated as [28]:

$$D_{ki}=\dot{L}_i(\tau_i)=\sum_{l=0}^{k}\frac{\prod_{j=0,j\neq i,l}^{k}\tau_k-\tau_j}{\prod_{j=0,j\neq i}^{k}\tau_i-\tau_j},k=1,...K,i=0,...,K \quad (23)$$

It is worth mentioning that the above equation is in the form of a set of algebraic constrains. Next, by using a Gauss–Radau quadrature, the original performance index is transformed as

$$J=h\left(\mathbf{X}_1,t_0,\mathbf{X}_{N+1},t_f\right)+\frac{t_0-t_f}{4}\sum_{k=1}^{N}w_k g\left(\mathbf{X}(\tau_k),\mathbf{U}(\tau_k),\tau_k;t_0,t_f\right) \quad (24)$$

where w_k, $(k=1,2,\ldots,N)$ are Legendre–Gauss–Radau weights. Also, the function g is the integrand in Eq. (16). The obtained equations, define a nonlinear programming problem. The resulted DOM problem formulation can then be solved numerically using any nonlinear programming problem. The provided result of this research is based on the SNOPT nonlinear solver of Stanford Company [28].

To apply the previously described approach, the GPOPS software package was developed by Rao et al. which has been utilized in this research [27], [29]-[32].

4. Computational results

In this section, a robot and a payload with the specifications shown in Table 1 has been taken into account. It is desired that TLRFM transfers the pre-captured payload from rest to a desired point of specified velocity, see Figure 2. The specifications of the robotic system and the desired mission have been provided in Table 2.

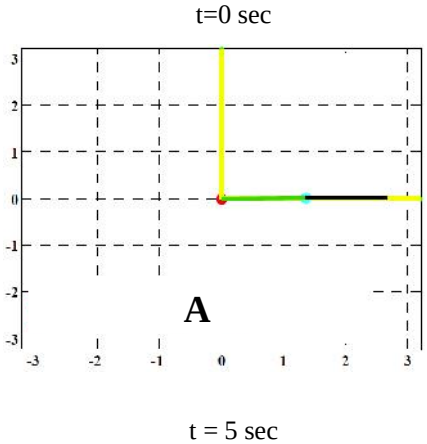

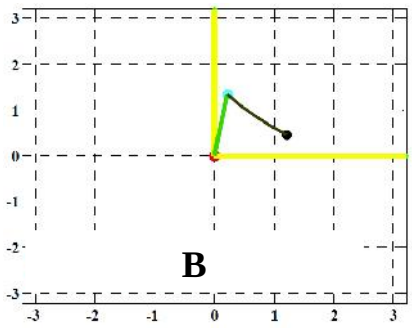

Figure 2. The considered DOM mission.

Based on the previous explanations, the efficiency of the designed controller in the DOM task is tested and deliberated in this section. Figures 3 and 4 show the robot first motor torque and the second one, respectively. Figure 5 presents the FL tip displacement in rotating frame. Also, the robot first motor angular position is demonstrated in Figure 6. In order to object launching, a 0 degree to approximately 81 degrees travel must be done precisely in 5 seconds, via the first motor, which Figure 6 confirms this claim. Additionally, Figure 7 depicts the second motor angular position. To object launching, the second motor should move from an initial angle of 0 degree to the final one that is approximately -118 degrees. This was realized and is demonstrated in Figure 7.

Figure 8 shows the tip positions, X and Y components, of the EE. In order to object launching, the EE of the robot must reach to the point $\mathbf{P_{sp}}=[1.3838 \quad 0.7676]^T(m)$ precisely at $t=5\ (\text{sec})$. Figure 8 confirms the ability of robot controller to meet the position conditions. The tip velocity components of the EE are shown in Figs. 9 and 10. The desired object velocity at the launch moment ($t=5$ sec) is $\mathbf{V_{sp}}=[-1 \quad -2]^T(m/\text{sec})$.

The obtained terminal velocities based on Figs. 9 and 10, confirm the desired conditions satisfaction for the velocity vector of the EE via the robot controller.

Table 3 demonstrates the final pose of the EE. By comparison of the actual values reported in Table 3 and related values of Table 2, the efficiency of the method is proven.

Table 2. The desired conditions of launching of the payload.

Phase	Start (Configuration A)	Launch (Configuration B)
t (sec)	0	5
EE position (m)	$\mathbf{P}_{st}=\begin{bmatrix}2.68\\0\end{bmatrix}$	$\mathbf{P}_{sp}=\begin{bmatrix}1.3838\\0.7676\end{bmatrix}$
EE velocity (m/s)	$\mathbf{V}_{st}=\begin{bmatrix}0\\0\end{bmatrix}$	$\mathbf{V}_{sp}=\begin{bmatrix}-1\\-2\end{bmatrix}$

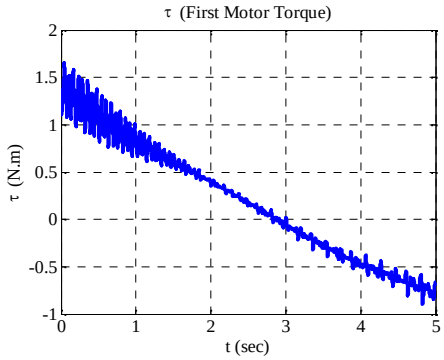

Figure 3. Applied torque by the robot first motor

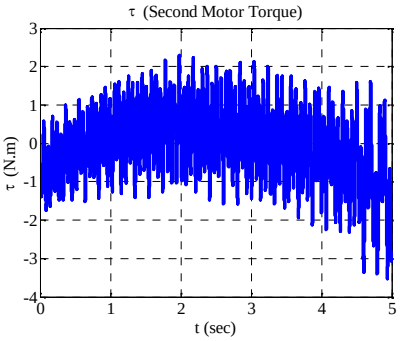

Figure 4. Applied torque by the robot second motor

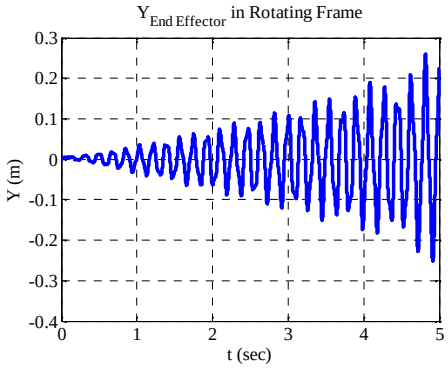

Figure 5. Tip displacement of the FL in rotating frame

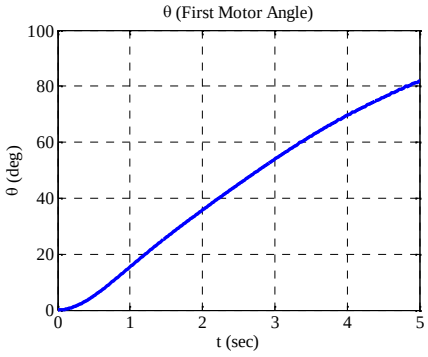

Figure 6. The first motor angular position

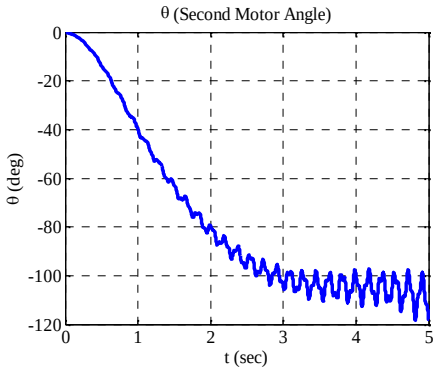

Figure 7. The second motor angular position

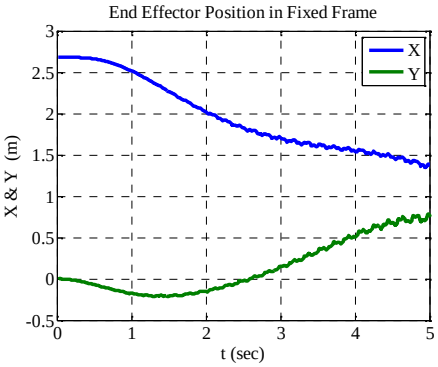

Figure 8. X and Y components of the EE position

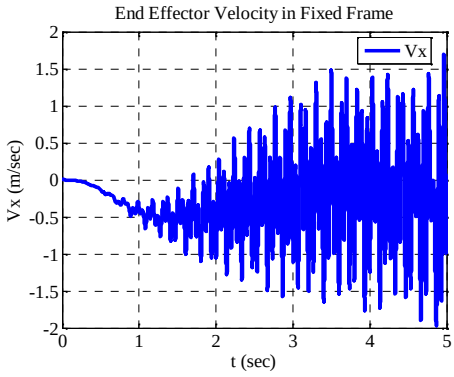

Figure 9. Velocity ($\dot{X}$) of the EE

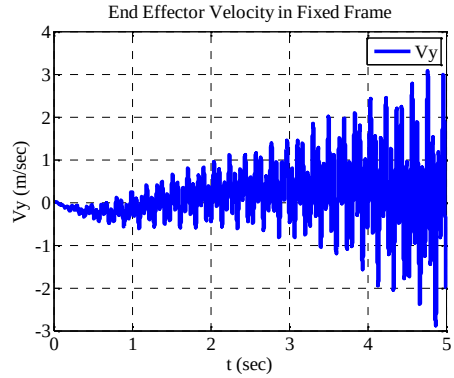

Figure 10. Velocity ($\dot{Y}$) of the EE

Table 3. The obtained conditions of launching of the payload.

Phase	Start (Configuration A)	Launch (Configuration B)
t (sec)	0	5
EE position (m)	$\mathbf{P}_{st}=\begin{bmatrix}2.68\\0\end{bmatrix}$	$\mathbf{P}_{sp}=\begin{bmatrix}1.3838\\0.7676\end{bmatrix}$
EE velocity (m/s)	$\mathbf{V}_{st}=\begin{bmatrix}0\\0\end{bmatrix}$	$\mathbf{V}_{sp}=\begin{bmatrix}-1\\-2\end{bmatrix}$

5. Composite Control Strategy

Although the object manipulation problem can be solved using the optimal control tool, it however suffers the lack of robustness against unforeseen disturbances and model uncertainties. To overcome this drawback, the previously proposed open-loop optimal controller is combined with proportional-Derivative-Integral (PID) controllers as illustrated in Figure 11.

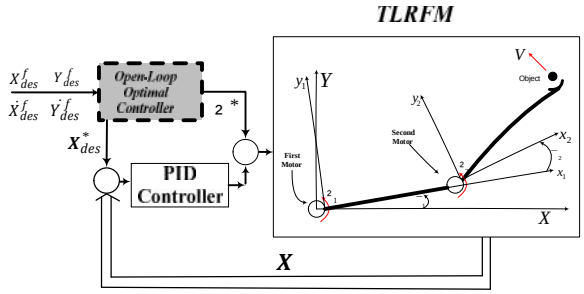

Figure 11. The proposed hybrid control structure

It is noteworthy that the developed control law has been formed based on partitioning the control signal into two parts, i.e. feedforwrad and feedback parts, $^{2}=^{2}_{feedforward}+^{2}_{feedback}$. Indeed, we have partitioned the controller into a model-based portion and a servo portion. The result is that the system's parameters appear only in the model-based portion (optimal controller) and that the servo portion (PID control) is independent of these parameters. The feedforward signal $^{2}_{feedforward}$ compensates for known major nonlinearities and known disturbances and reduces the system so that it appears to be an almost linear system. In other words, the optimal control portion of the control law has the effect of making the system appear as a near-linear system, so the design of the servo portion is very simple.

It is worth mentioning that in nonlinear control, the concept of feedback plays a fundamental role in controller design, as it does in linear control. However, the importance of feedforward is much more conspicuous than in linear control. Feedforward is used to cancel the effects of known disturbances and provide anticipative actions in tracking tasks. Very often it is impossible to control a nonlinear system stably without incorporating feedforward action in the control law [23, page 199].

The effect of adding the closed-loop controller to the previously open-loop optimal one can be observed in Figures 12-19. The effect of an external disturbance on system response can be seen in Figures 12-15. The magnitude of this disturbance is considered to be 10 percentages of the controlled input magnitude. As seen while the response of open-loop optimal control has significantly deviated from desired one, the hybrid controller can preserve the system desired behavior and attenuate the effects of external disturbance. As shown in Figures 12-15, the hybrid controller can effectively direct the robot to the desired terminal point and therefore the payload can successfully be thrown.

The effect of model uncertainties on the response of the system has been illustrated in Figures 16-19. While the response of open and closed-loop controllers are close in the level of position, their responses in the level of velocity are far apart. In other words, the closed-loop controller, in contrast to the open-loop, can effectively provide the terminal desired position and velocity of the payload at the final time, even in the presence of model uncertainty.

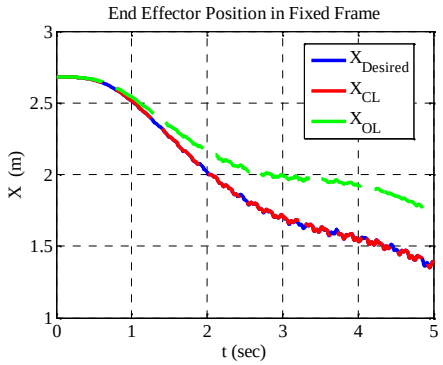

Figure 12. Comparison of open-loop versus hybrid one in terms of end-effector position along horizontal axis in the presence of external disturbances

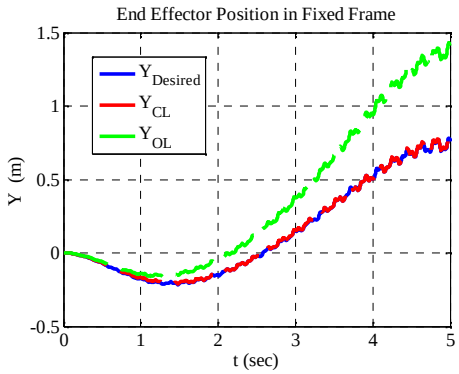

Figure 13. Comparison of open-loop versus hybrid one in terms of end-effector position along vertical axis in the presence of external disturbances

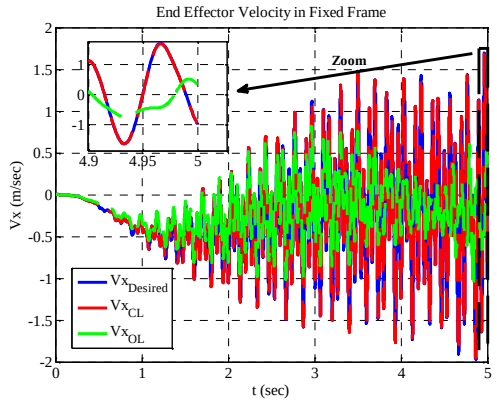

Figure 14. Comparison of open-loop versus hybrid one in terms of end-effector velocity along horizontal axis in the presence of external disturbances

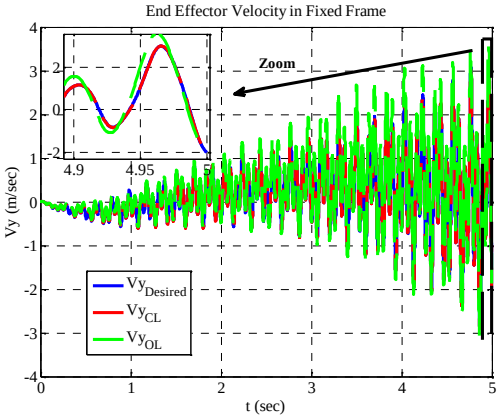

Figure 15. Comparison of open-loop versus hybrid one in terms of end-effector velocity along vertical axis in the presence of external disturbances

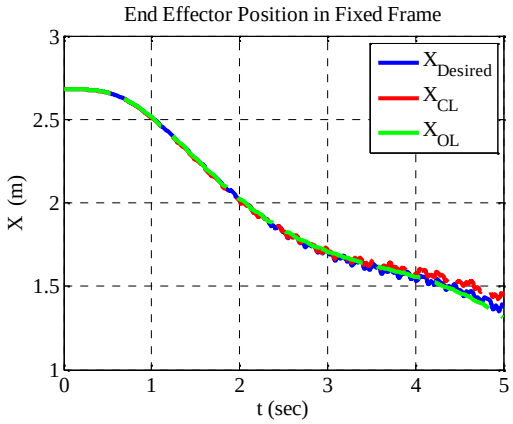

Figure 16. Comparison of open-loop versus hybrid one in terms of end-effector position along horizontal axis in the presence of model uncertainties

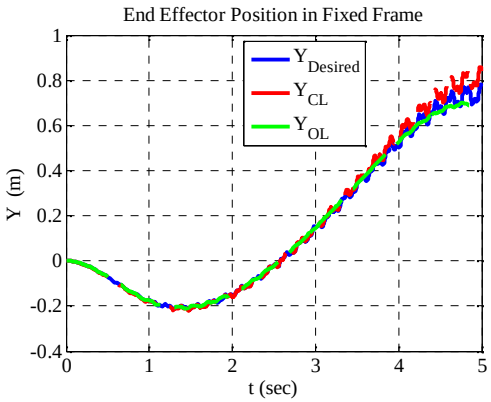

Figure 17. Comparison of open-loop versus hybrid one in terms of end-effector position along vertical axis in the presence of model uncertainties

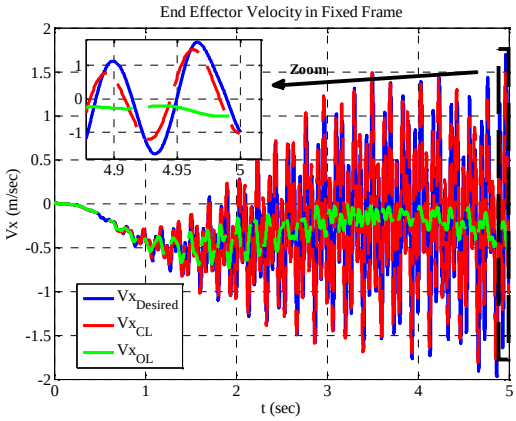

Figure 18. Comparison of open-loop versus hybrid one in terms of end-effector velocity along horizontal axis in the presence of model uncertainties

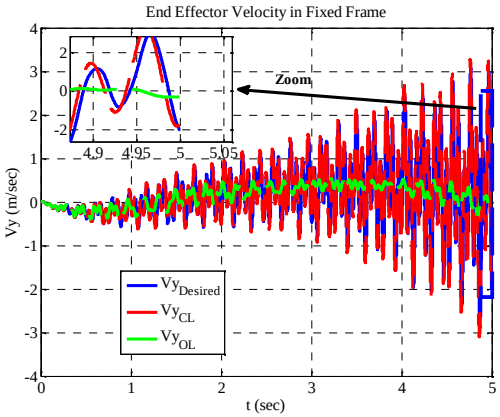

Figure 19. Comparison of open-loop versus hybrid one in terms of end-effector velocity along vertical axis in the presence of model uncertainties

6. Conclusion

The purpose of the present research is to find the optimal trajectories and control input of TLRFM for performing DOM tasks. To this end, the powerful optimal nonlinear control method is exploited. This research investigates DOM mission especially with a special aim of launching an object to a specified position in the two dimensional plane with the predetermined desired velocity vector during the limited and specified time interval. The controller design problem formulated as a complicated nonlinear optimal control problem. The pseudospectral method, which is based on direct collocation method, was employed to numerical solution of the resulted problem. To this end, the state and control were approximated using global polynomials and collocation of the differential-algebraic equations is performed at orthogonal collocation points, in Pseudospectral method. The achieved nonlinear programming problem based on Pseudospectral method, was solved using SNOPT nonlinear solver. To provide the robustness of the controller, a closed-loop PID based controller structure was added to the original optimal controller. The obtained simulation results support the usefulness and efficiency of the developed scheme in solving the DOM problem employing TLRFMs.

References

[1] H. H. Lee and Y. Liang, "A coupled-sliding-surface approach for the robust trajectory control of a horizontal two-link rigid/flexible robot", *International Journal of Control*, Vol. 80(12), (2007), pp. 1880-1892.

[2] J. F. Peza-Solis, G. Silva-Navarro and R. Castro-Linares, "Control of a rigid-flexible two-link robot using passivity-based and strain-feedback approaches", 7th International Conference on Electrical Engineering, Computing Science and Automatic Control (CCE 2010), Tuxtla Gutiérrez, Chiapas, México, (2010), pp. 476-481.

[3] A. Abe, "Trajectory planning for residual vibration suppression of a two-link rigid-flexible manipulator considering large deformation", *Mechanism and Machine Theory*, Vol. 44, (2009), pp. 1627–1639.

[4] L. Z. Shi and M. B. Trabia, "Comparison of distributed PD-like and importance based fuzzy logic controllers for a two-link rigid-flexible manipulator", *Journal of Vibration and Control*, Vol. 11, (2005), pp. 723–747.

[5] S. Akella, W. H. Huang, K. M. Lynch and M. T. Mason, "Sensorless parts orienting with a one-joint manipulator", IEEE International Conference on Robotics and Automation, Vol. 3, (1997), pp. 2383-2390.

[6] M. Erdmann, "An exploration of nonprehensile two-palm manipulation", International Journal of Robotics Research, Vol. 17(5), (1998), pp. 485-503.

[7] Y. Maeda, T. Nakamura and T. Arai, "Motion planning of robot fingertips for graspless manipulation", Proceeding of IEEE International Conference on Robotics and Automation, (2004), pp. 2951 – 2956.

[8] Y. Maeda and T. Arai, "Planning of graspless manipulation by a multifingered robot hand", *Advanced Robotics*, Vol. 19(5), (2005), pp. 501-521.

[9] . K. Miyazawa, Y. Maeda and T. Arai, "Planning of graspless manipulation based on rapidly-exploring random trees", Proceeding of IEEE International Symposium on Assembly and Task Planning: From Nano to Macro Assembly and Manufacturing, (2005), pp. 7-12.

[10] A. Akbarimajd and M. N. Ahmadabadi, "Manipulation by juggling of planar polygonal objects using two 3-DOF manipulators", Proceeding of IEEE/ASME International Conference of Advanced Intelligent Mechatronics, (2007), pp. 1-6.

[11] S. Akella, W. H. Huang, K. M. Lynch and M. T. Mason, "Planar manipulation on a conveyor with a one joint robot", the 7th International Symposium on Robotics Research, (1995), pp. 265-277.

[12] K. M. Lynch and M. T. Mason, "Stable pushing: mechanics, controllability, and planning", *The International Journal of Robotic Researches*, Vol. 15(6), (1996), pp. 533-556.

[13] K. M. Lynch and M. T. Mason, "Dynamic nonprehensile manipulation: controllability, planning, and experiments", *The International Journal of Robotics Research*, Vol. 18(1), 1999,pp. 64-92.

[14] T. Tabata and Y. Aiyama, "Tossing manipulation by 1 degree of-freedom manipulator", Proceeding of the IEEE/RSJ International Conference on Intelligent Robots and Systems, (2001), pp. 132−137.

[15] B. Beigzadeh, M. N. AhmadAbadi and A. Meghdari, "Two dimensional dynamic manipulation of a disc using two manipulators", Proceeding of IEEE International Conference on Mechatronics and Automation, (2006), pp. 1191−1196.

[16] A. Akbarimajd, M. N.Ahmadabadi and B. Beigzadeh, "Dynamic object manipulation by an array of 1-DOF manipulators: Kinematic modeling and planning", Robotics and Autonomous Systems Vol. 55(6), 2007, pp. 444–459.

[17] H. Miyashita, T. Yamawaki and M. Yashima, "Control for throwing manipulation by one joint robot", Proceeding of IEEE International Conference on Robotics and Automation, (2009), pp. 1273-1278.

[18] K. Tahara, K. Maruta and M. Yamamoto, "External sensorless dynamic object manipulation by a dual soft-fingered robotic hand with torsional fingertip motion", Proceeding of IEEE International Conference on Robotics and Automation, (2010), pp. 4309-4314.

[19] K. Tahara, S. Arimoto and M. Yoshida, "Dynamic object manipulation using a virtual frame by a triple soft-fingered robotic hand", Proceeding of IEEE International Conference on Robotics and Automation, (2010), pp. 4322-4327.

[20] B. Tarvirdizadeh and A. Yousefi-Koma, "Dynamic object manipulation by a flexible robotic arm; theory and experiment", *International Journal of Robotics and Automation*, Vol. 27(3), 2012, pp. 263-275.

[21] G. G. Rigatos, "Model-based and model-free control of flexible-link robots: A comparison between representative methods", *Applied Mathematical Modelling*, Vol. 33(10), (2009), pp. 3906–3925.

[22] M. Vakil, R. Fotouhi and P. N. Nikiforuk, "Maneuver control of the multilink flexible manipulators", *International Journal of Non-Linear Mechanics*, Vol. 44(8), (2009), pp. 831-844.

[23] D. Wang and M. Vidyasagar, "Transfer functions for a single flexible link", Proceedings of IEEE International Conference on Robotics and Automation, Vol. 2, (1989), pp. 1042 - 1047

[24] X. Zhang, W. Xu and S. S. Nair, "Comparison of some modeling and control issues for a flexible two link manipulator", *ISA Transactions*, Vol. 43, (2004), pp. 509–525.

[25] S. Choura and A. S. Yigit, "Control of a two-link rigid-flexible manipulator with a moving payload mass", *Journal of Sound and Vibration*, Vol. 243(5), (2001), pp. 883-897.

[26] R. I. Milford and S. F. Asokanthan, "Configuration dependent eigenfrequencies for a two-link flexible manipulator: experimental verification", *Journal of Sound and Vibration*, Vol. 222(2), (1999), pp. 191-207.

[27] A. V. Rao, D. A. Benson and G. T. Huntington, Algorithm 902: GPOPS, "A MATLAB Software for Solving Multiple-Phase Optimal Control Problems Using the Gauss Pseudospectral Method", *ACM Transactions on Mathematical Software*, Vol. 37(2), (2010), pp. 22-38.

[28] P. E. Gill, W. Murray and M. A. Saunders, User's Guide for SNOPT Version 7: Software for Large Scale Nonlinear Programming, 2006.

[29] D. A. Benson and G. T. Huntington, T. P. Thorvaldsen and A. V. Rao, "Direct Trajectory Optimization and Costate Estimation via an Orthogonal Collocation Method", *Journal of Guidance, Control, and Dynamics*, Vol. 29(6), (2006), pp. 1435-1440.

[30] D. Garg, M. A. Patterson, C. L. Darby, C. Francolin, G. T. Huntington, W. W. Hager and A. V. Rao, "Direct Trajectory Optimization and Costate Estimation of Finite-Horizon and Infinite-Horizon Optimal Control Problems Using a Radau Pseudospectral Method", *Computational Optimization and Applications*, Vol. 49(2), (2011), pp. 335-358.

[31] D. A. Benson and G. T. Huntington, "A Unified Framework for the Numerical Solution of Optimal Control Problems Using Pseudospectral Methods", *Automatica*, Vol. 46(11), (2010), pp. 1843-1851.

[32] D. Garg, M. A. Patterson, W. W. Hager, A. V. Rao, D. A. Benson and G. T. Huntington, "A Unified Framework for the Numerical Solution of Optimal Control Problems Using Pseudospectral Methods", *Automatica*, Vol. 46(11), (2010), pp. 1843-1851.

[33] J. J. E. Slotine and W. Li, "Applied Nonlinear Control", Prentice-Hall Inc., Englewood Cliffs, New Jersey, (1991).

Biography

Bahram Tarvirdizadeh received the B.Sc. degree in Mechanical engineering from K.N. Toosi University of Technology, Iran, in 2004. He received his M.Sc. and Ph.D. degree in the same field from University of Tehran, Iran, in 2006 and 2012, respectively. He is assistant professor of faculty of new sciences and technologies of university of Tehran, recently. His main research interests include robotics, dynamic object manipulation, non-linear dynamics, vibration and control, non-linear optimal control, experimental mechanics and controller, and circuit design for actual dynamic systems.

Khalil Alipour received his BS, MS, and PhD degrees all with honors in Mechanical Engineering in 2002, 2004, and 2010, respectively. Currently, he is an assistant professor with the Faculty of New Sciences and Technologies at University of Tehran. He teaches courses in the areas of robotics, dynamics, automatic control, analysis, and synthesis of mechanisms. His research interests are in the areas of dynamics modeling, automatic control, motion/path planning of robotic systems, and tip-over stability analysis of mobile robots. He has published more than 60 articles in national and international journals and conference proceedings.